

available at www.sciencedirect.comjournal homepage: www.elsevier.com/locate/jhydrol

Spatial and temporal rainfall variability in mountainous areas: A case study from the south Ecuadorian Andes

Wouter Buytaert^{a,b,*}, Rolando Celleri^c, Patrick Willems^c, Bert De Bièvre^b, Guido Wyseure^a

^a *Laboratory for Soil and Water Management, Katholieke Universiteit Leuven, Celestijnenlaan 200 E, 3001 Leuven, Belgium*

^b *Programa para el Manejo del Agua y del Suelo, Universidad de Cuenca, Ecuador*

^c *Hydraulics Laboratory, Katholieke Universiteit Leuven, 3001 Leuven, Belgium*

Received 20 July 2005; received in revised form 16 February 2006; accepted 23 February 2006

KEYWORDS

Rainfall variability;
Mountain environments;
Interpolation;
Kriging;
Thiessen;
Ecuador

Summary Particularly in mountain environments, rainfall can be extremely variable in space and time. For many hydrological applications such as modelling, extrapolation of point rainfall measurements is necessary. Decisions about the techniques used for extrapolation, as well as the adequacy of the conclusions drawn from the final results, depend heavily on the magnitude and the nature of the uncertainty involved. In this paper, we examine rainfall data from 14 rain gauges in the western mountain range of the Ecuadorian Andes. The rain gauges are located in the western part of the rio Paute basin. This area, between 3500 and 4100 m asl, consists of mountainous grasslands, locally called páramo, and acts as major water source for the inter-Andean valley. Spatial and temporal rainfall patterns were studied. A clear intraday pattern can be distinguished. Seasonal variation, on the other hand, is low, with a difference of about 100 mm between the driest and the wettest month on an average of about 100 mm month⁻¹, and only 20% dry days throughout the year. Rain gauges at a mutual distance of less than 4000 m are strongly correlated, with a Pearson correlation coefficient higher than 0.8. However, even within this perimeter, spatial variability in average rainfall is very high. Significant correlations were found between average daily rainfall and geographical location, as well as the topographical parameters slope, aspect, topography. Spatial interpolation with thiessen gives good results. Kriging gives better results than thiessen, and the accuracy of both methods improves when external trends are incorporated.

© 2006 Elsevier B.V. All rights reserved.

* Corresponding author. Present address: Department of Environmental Sciences, Lancaster University, UK. Tel.: +32169735.
E-mail address: w.buytaert@lancaster.ac.uk (W. Buytaert).

Introduction

Assessing rainfall variability is a frequent practice in hydrology. An important application is the estimation of total rainfall over an area, e.g., a catchment, as an input for hydrological models. Precipitation is in many cases the most important input factor in hydrological modelling (Beven, 2001b). However, this input is subject to uncertainty, as a result of measurement errors, systematic errors in the interpolation method and stochastic error due to the random nature of rainfall. These input errors propagate through the model and have a direct impact on the accuracy of the final predictions. Therefore, quantification and a good knowledge of the uncertainty in the hydrological input data is essential for a correct interpretation of modelling results (Jakeman and Hornberger, 1993; Beven, 2001a).

Nevertheless, accurate estimation of the spatial distribution of rainfall and extrapolation of point measurements over large areas is complicated. This is especially true in mountainous environments. In mountain regions, in addition to the stochastic nature of rainfall, the precipitation pattern may be influenced by the irregular topography. The large variability in altitude, slope and aspect may increase variability by means of processes such as rain shading and strong winds. The best method to improve the quality of spatial rainfall estimation is to increase the density of the monitoring network. However, this is very costly, and in many cases practically infeasible. And even for dense networks, interpolation remains necessary in order to calculate

the total rainfall over a certain area (Goovaerts, 2000). Therefore, both the design of an adequate monitoring network and choice of an interpolation method require insight in the patterns of rainfall variability and the sources of uncertainty.

In this study, we analyse daily rainfall series from 14 rain gauges located in the páramo of the Paute river basin, south Ecuador (Fig. 1). The páramo is a high altitude neotropical grassland ecosystem, located between the continuous forest border (about 3500 m asl) and the permanent snow line (about 5000 m asl) of the northern Andes (Mena and Medina, 2001; Hofstede et al., 2003). The páramo forms a discontinuous belt that stretches from northern Peru over Ecuador and Colombia to Venezuela and covers about 35,000 km² (Luteyn, 1999; Hofstede et al., 2003). In general, the climate is cold and wet, but a large spatial variability is present, with precipitation ranging from <1000 mm up to >4000 mm (Sarmiento, 1986; Hofstede et al., 2003; Luteyn, 1999; Hofstede et al., 2003). The Andes has a very complex precipitation pattern, influenced by both the Pacific and the Amazon basin. The eastern slopes are dominated by perennially wet easterly trade winds originating over the tropical Atlantic and Amazon basin. In the northernmost Andes of Venezuela, northern Colombia and Costa Rica, the north-east Trade Winds give rise to a marked dry season. The western slopes of Colombia and Ecuador are influenced by an intertropical convergence zone (ITCZ) over the eastern Pacific (Vuille et al., 2000). The ITCZ is responsible for a continuous moisture in the form of rain, clouds and fog, as a

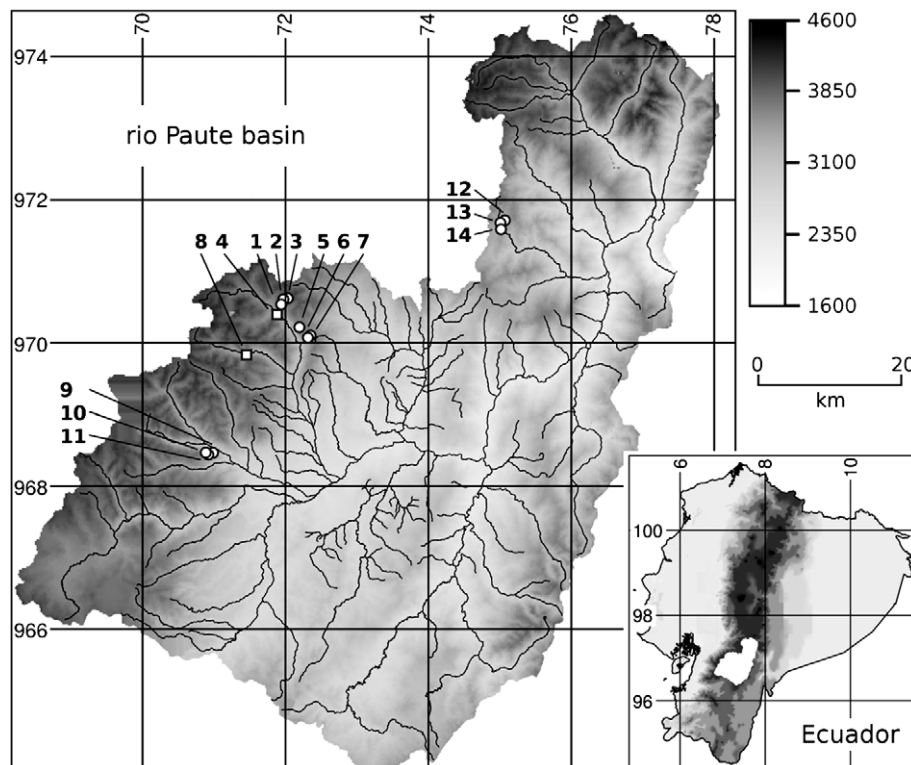


Figure 1 Geographical map of the study region. 1, 2, 3 = Huagrahuma microcatchment; 5, 6, 7 = Soroché microcatchment; 9, 10, 11 = Mazan microcatchment, 12, 13, 14 = Ningar microcatchment; 4 = Chanlud; 8 = Labrado. □ = dam sites of Chanlud (4) and Labrado (8). The rain gauges in the microcatchments are of the tipping bucket type, while these at the dam sites are daily data from ETAPA. Coordinates are in 10⁴ UTM on the detailed map and 10⁵ UTM on the overview map.

result of the orographic uplift. Finally, the páramos on the eastern slopes of south Ecuador and north Peru are influenced by dry and cool airmasses from the Humboldt Current, and are therefore much dryer (Sarmiento, 1986; Luteyn, 1999). The inter-Andean valleys between the western and the eastern mountain range experience a varying influence from oceanic and continental airmasses, resulting in a bimodal seasonal distribution. These complex interactions, combined with the irregular topography and the large differences in slope, aspect and elevation, result in strongly varying weather patterns at local level.

The study is aimed at improving our understanding of the major sources of variation and uncertainty in small scale rainfall interpolation in mountainous environments. This is achieved by means of a spatial and temporal characterisation and correlation analysis of the daily rainfall series. In a second part, the difference in uncertainty between two interpolation methods that differ strongly in complexity, Thiessen polygons and kriging, is assessed by means of cross validation. This allows us to evaluate the amount of complexity allowed in interpolation, in view of the available data.

Furthermore, the study aims at a better insight in the hydrology of the páramo ecosystem. Because of the difficulties involved in ground water extraction, surface water from the ecosystem is a vital water source for the inter-Andean region. Water is used for agricultural and urban purposes, and for energy production in hydropower facilities. Large cities such as Bogota and Quito extract more than 90% of their water from the páramo (FAO, 2000; UAESPNN, 2000). In the studied area, surface water from the páramo is the only water source for the city of Cuenca, (500,000 inhabitants) and supplies water to the reservoirs of El Labrado and Chanlud, generating together 38.4 MW (ETAPA, 2004). One of the major reasons for this reliance is the large and sustained base flow in the rivers coming from the páramo. The mechanism behind this water regulation is largely unknown, but the lack of seasonal variability in rainfall may be one of the major causes (Buytaert et al., 2005). At present, quantitative data about these variations are very scarce. The same problem exists for the total amount of rainfall in the páramo. Despite its importance as a water supplier, the total available water, as well as the water balance, have never been quantified.

Finally, it is expected that global climate changes will have a strong impact on the hydrology and climate of the páramo. It is well known that mountain environments are particularly vulnerable for climatic changes (IPCC, 2001; Beniston, 2003; Messerli et al., 2004). In the páramo, specifically the western slopes, the influence of the El Niño/Southern Oscillation may intensify these impacts. Given the socio-economic and ecological importance of the páramo as a water supplier, detailed long time monitoring of possible changes is necessary. This study intends to contribute to a reference base for future observations and analysis.

Study area

In Ecuador, the Andes consists of two parallel mountain ranges separated by a tectonic depression. The study area is located in the western mountain range of south Ecuador,

and forms a part of the Paute basin (Fig. 1). The climatic pattern in the western mountain range is influenced by the Pacific coastal regime from the west, and the continental and tropical Atlantic air masses from the east (Vuille et al., 2000). The resulting precipitation pattern is bimodal, with a major dry season in August to September and a less pronounced dry season around December to February. However, as is typical for intertropical regions, yearly fluctuations are small (Sarmiento, 1986; Hofstede et al., 2003).

In the Paute basin, the neotropical Andean ecosystem páramo extends from about 3300 to 4620 m, which is the highest point in the basin. It is a remote and desolate area, characterised by a low grass vegetation consisting of tussock grass species (mostly *Calamagrostis* spp., *Festuca* spp., *Stipa* spp.) and scarcely scattered patches of individual, small and gnarled growing trees, particularly of the genus *Polylepis* and *Gynoxys* (Hedberg, 1992; Luteyn, 1992). The lack of intensive human activities in most páramos guarantees high water quality. Annually, more than 50 million m³ water is extracted from the study region. This water is used by the city of Cuenca, which is the third largest city of Ecuador and the capital of the province of Azuay.

Materials and methods

Twelve rain gauges were installed in four microcatchments in the western mountain range: Mazan, Soroche, Huagrahuma and Ningar (Fig. 1). Catchment selection was done to study the impact of land use on the hydrology. All rain gauges are tipping bucket gauges with a resolution of 0.2 mm, except at Mazan, where the resolution is 0.254 mm. The tipping bucket data were converted to daily rainfall series. These data were completed with daily rainfall measurements made by ETAPA (Cuenca's public company for drinking water) at the dam sites of Chanlud and Labrado. The resolution of these gauges is 0.5 mm day⁻¹. After a certain monitoring time, rain gauges were interchanged to analyse systematic differences in recordings, which proved to be neglectable. The area covered by the rain gauges is about 650 km², giving a network density of slightly less than 1 per 50 km². It has to be noted, however, that the rain gauges are clustered, allowing for an analysis at a smaller scale (Fig. 1).

The GIS data are derived from digitised elevation contours with an interval of 20 m and a scale of 1:25000. Using regular spline with tension (Mitasova and Mitas, 1993), elevation, slope and aspect maps with a resolution of 25 m were generated.

The impact of the topography on the average daily rainfall was assessed with linear regression. The average daily rainfall was split per month and the monthly data were correlated with altitude, aspect, slope and east and north coordinates. The aspect was split in quadrants (N, W, E, S), on which factor analysis of variance (ANOVA) was done.

Two methods for the interpolation of the daily rainfall average are used: Thiessen polygons and kriging. The methods are chosen because they represent two ends in a spectrum of interpolation methods. Thiessen is a simple and straightforward method. Each interpolated location is given the value of the closest measurement point, resulting in a typical polygonal pattern and discontinuities at the borders

of the polygons. Kriging on the other hand is an advanced, computationally intensive, geostatistical estimation method (for both methods see e.g., Burrough and McDonnell, 1998; Goovaerts, 2000; Haan, 2002). In both methods, the results of the multiple regression results are incorporated. For Thiessen, the data were normalised, based on the relation of the mean daily rainfall with the topographical parameters (Table 2). After the interpolation, the normalisation was reversed. For kriging, universal kriging was applied using the *R* implementation of *gstat* (Pebesma, 2004).

The availability of daily rainfall series has a specific advantage for kriging. In most applications, only one measurement (e.g., average rainfall) is available for each observation point. The experimental semivariogram $\hat{\gamma}(h)$ is then estimated by means of the differences between each data pair:

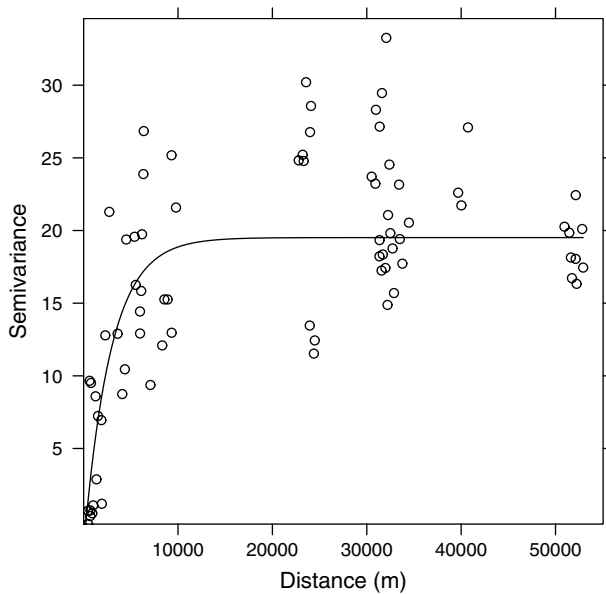


Figure 2 The semivariogram cloud for daily rainfall in the Paute basin, with a fitted exponential model.

$$\hat{\gamma}(h) = \frac{1}{2N(h)} \sum_{i=1}^{N(h)} (z_i - z_{i+h})^2 \quad (1)$$

where $N(h)$ is the number of points separated by a distance h , and z_i is the average daily rainfall at point i (Haan, 2002). When series are available at each point, the experimental semivariogram can be calculated by:

$$\hat{\gamma}(h) = \frac{\text{Var}(z_i - z_{i+h})}{2} = \text{Var}(z_i) + \text{Var}(z_{i+h}) - 2\text{Cov}(z_i, z_{i+h}) \quad (2)$$

which resembles more closely the definition of semivariance (Haan, 2002). When relatively few locations are available, such as in this study, this greatly improves semivariogram estimation (Fig. 2).

Results and discussion

Statistical distribution

A summary of the data and the rain gauge characteristics is given in Table 1. The cumulative rainfall in the gauged catchments is given in Fig. 3. For the statistical distribution function of daily rainfall, a mixed population is generally suggested (Hyndman and Grunwald, 2000). In a mixed population, a discrete component at zero is used for the prediction of dry days. This is combined with a positive continuous component, mostly a lognormal or gamma function, for the prediction of the amount of rainfall at wet days.

In the páramo, however, rainfall is characterised by short, frequent, low volume events, and an equal distribution over the year (Fig. 3). As a result, days without rain (or, with less than 0.2 mm of rain if the resolution of the rain gauges is taken into account) do not occur very frequently: on average only 24% of the days during the monitored period. This observation makes it reasonable to omit the discrete component for simplicity reasons. Due to the occurrence of frequent low volume events, daily rainfall can be considered as the sum of a few, short ‘‘storm’’ events, which are commonly described using a Weibull dis-

Table 1 Major characteristics of the rain gauge sites used in this study

| Location | Min (mm) | Median (mm) | Mean (mm) | Max (mm) | Altitude (m) | Aspect (°N) | Slope (%) | <i>n</i> (days) |
|----------|----------|-------------|-----------|----------|--------------|-------------|-----------|-----------------|
| 1 | 0.0 | 1.40 | 3.44 | 40.6 | 3700 | 200 | 16.2 | 1465 |
| 2 | 0.0 | 1.80 | 4.28 | 52.4 | 3815 | 307 | 43.1 | 1486 |
| 3 | 0.0 | 1.40 | 3.27 | 30.8 | 3819 | 215 | 2.9 | 1408 |
| 4 | 0.0 | 1.00 | 3.19 | 36.5 | 3443 | 42 | 11.6 | 577 |
| 5 | 0.0 | 1.60 | 3.27 | 27.0 | 3683 | 216 | 5.4 | 444 |
| 6 | 0.0 | 1.40 | 3.10 | 38.2 | 3661 | 168 | 2.2 | 585 |
| 7 | 0.0 | 1.60 | 3.34 | 38.0 | 3541 | 228 | 4.1 | 479 |
| 8 | 0.0 | 1.00 | 3.67 | 33.0 | 3440 | 78 | 13.3 | 577 |
| 9 | 0.0 | 1.00 | 2.81 | 23.6 | 3375 | 312 | 17.9 | 330 |
| 10 | 0.0 | 1.27 | 3.12 | 23.4 | 3438 | 55 | 5.5 | 328 |
| 11 | 0.0 | 1.27 | 2.96 | 24.1 | 3621 | 43 | 34.7 | 329 |
| 12 | 0.0 | 1.20 | 3.72 | 51.4 | 3420 | 146 | 15.1 | 963 |
| 13 | 0.0 | 1.20 | 3.33 | 40.2 | 3317 | 219 | 0.9 | 902 |
| 14 | 0.0 | 1.20 | 3.39 | 40.2 | 3339 | 225 | 19.1 | 969 |

Min, median, mean and max are, respectively, the minimum, median, mean and maximum daily rainfall at the location. *n*, number of daily rainfall data available for the location.

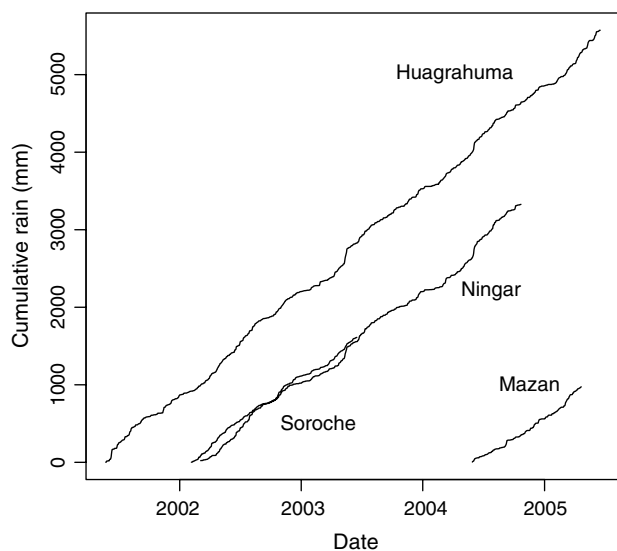


Figure 3 Cumulative daily rainfall in each of the studied microcatchments. For each line, the daily rainfall was averaged over the rain gauges located in the respective catchment: 1, 2, 3 = Huagrahuma; 5, 6, 7 = Soroché; 9, 10, 11 = Mazan; 12, 13, 14 = Ningar.

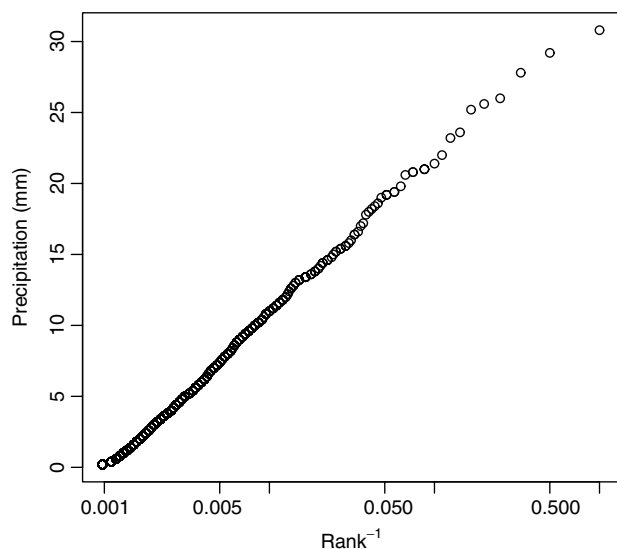


Figure 4 Inverse ranking of the daily rainfall values at rain gauge 3. Linearity on the semilogarithmic plot (which can be observed here) is a good indication for an exponential distribution of the daily rainfall.

tribution (Willems, 2001). Indeed, an exponential function, which can be considered as a special case of the Weibull distribution, proves to be an adequate estimator for the daily rain volume distribution (Fig. 4).

Temporal variability

Tropical alpine ecosystems differ sharply from similar ecosystems at middle or high latitudes in having very reduced monthly variation in solar radiation. As a result, climatic

differences are generally much smaller too. However, under the influence of trade winds, with their cyclic displacement across the equator, a strong variation in rainfall seasonality may occur at certain locations, such as the páramos of Venezuela and northern Colombia (e.g., Sierra Nevada de Santa Marta). In páramos under influence of the equatorial trough, such as the study region, seasonal variability is much smaller (Sarmiento, 1986). The western Paute basin experiences a major dry season from August to October and a shorter, but more pronounced dry season from December to February (Fig. 5). However, the second wet period in November is not very pronounced and small compared to the main wet season from May to July. The resulting seasonal pattern is therefore somewhere between monomodal and bimodal. The close resemblance of the seasonal pattern of Mazan with the other locations is surprising. As Mazan is located more to the east, a stronger impact of the monomodal Amazon basin would be expected, where the driest season occurs from November to February. Nevertheless, the second peak of the bimodal Pacific distribution, in November, is still clearly present in this catchment.

However, despite these annual variations, few significant trends can be detected in the autocorrelation function (Fig. 6). The lag time for a significant autocorrelation is 3 days, which is very short and highlights the high degree of randomness in rainfall generation.

Intradaily rainfall distribution shows a conspicuous trend (Fig. 7). This is not surprising in mountain environments. Páramos are known for the sudden changes in weather and the high diurnal temperature fluctuations. Temperature is close to freezing at night but may increase up to 25 °C during the day, a cycle which is commonly referred to as "summer every day and winter every night" (Hedberg, 1964). The high diurnal amplitude in temperature is a result of the large solar radiation in tropical mountainous regions. Therefore, mornings are often free of clouds and with a

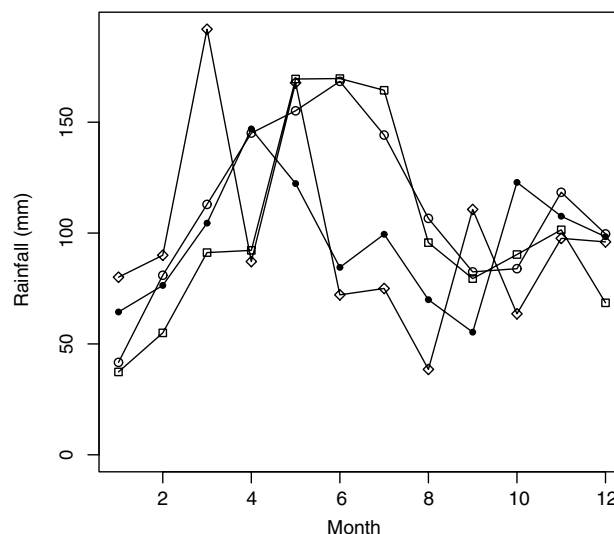


Figure 5 Annual distribution of the average monthly rainfall at the studied microcatchments. The major wet season runs from May to July, while the second wet season in November is hardly distinguishable. ● = Soroché; ○ = Huagrahuma; ◇ = Mazan; □ = Ningar.

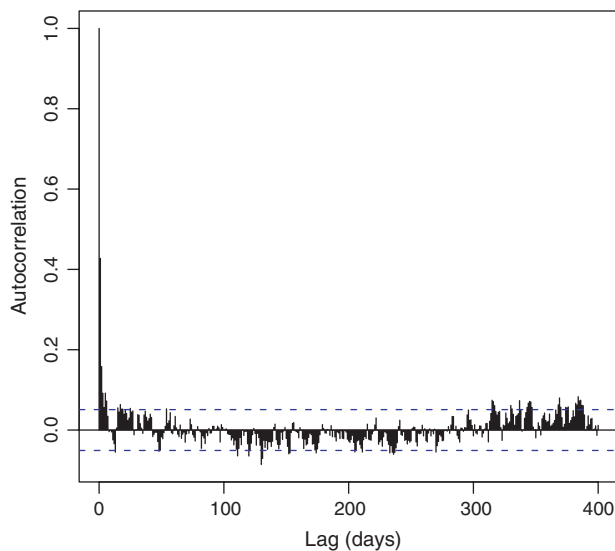


Figure 6 Autocorrelation of the time series of rain gauge 3, located in Huagrahuma microcatchment. The dashed line represents the limit of significant correlation on a 95% confidence coefficient. The autocorrelation time is 3 days.

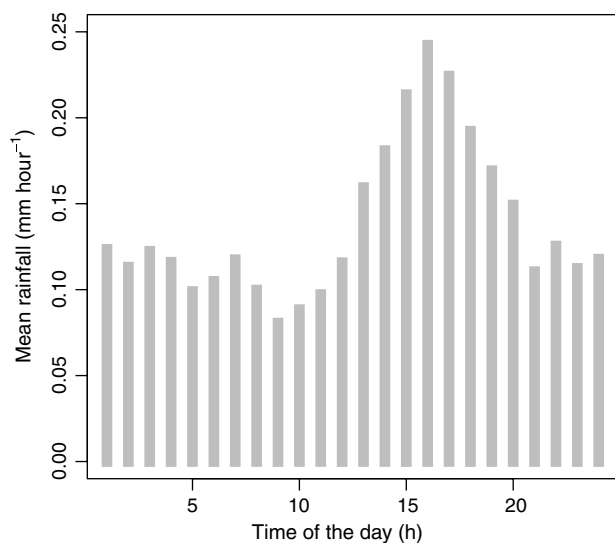


Figure 7 Intraday variation in rainfall of rain gauge 3 (Huagrahuma microcatchment). The sum of the values equals the average daily rainfall (3.27 mm). The timeseries used is 2001–2005.

clear sky. In the afternoon, the energy input in the lower atmosphere induces convective and orographic uplift, bringing an increased cloud cover with rain and fog. During the evening, clearing occurs (Luteyn, 1999).

Spatial variability

The correlogram is given in Fig. 8. A logarithmic model is fitting the correlogram well, but two major groups are observed. Rain gauges at a mutual distance of less than 4000 m are strongly correlated, with a Pearson correlation coefficient (R^2) between 0.80 and 0.98. At distances larger

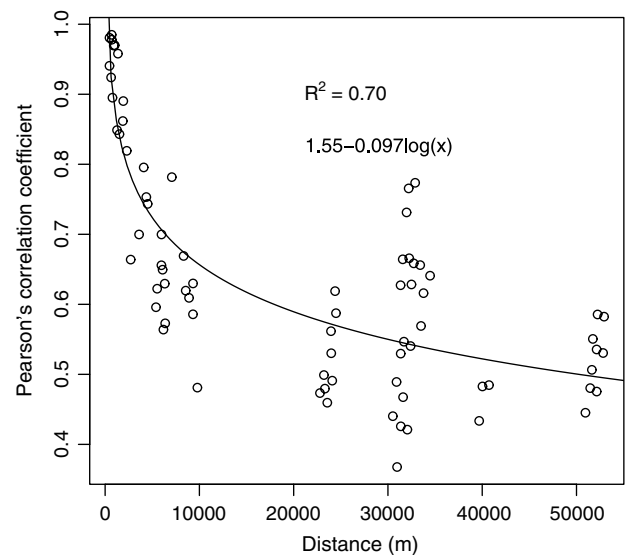


Figure 8 Spatial correlation between the rain gauges used in this study, with a logarithmic trendline. Two major groups can be observed. Correlation is much stronger between rain gauges at a mutual distance of less than 4000 m.

than 4000 m, the correlation strongly decreases to a range of roughly 0.4–0.8. Here, the correlation is far less dependant on the actual distance. We may conclude that the span of most rainfall events does not exceed about 4000 m. This is rather small and typical for regions with an irregular topography. Ridges and peaks may act as a natural barrier for storms, and differences in aspect and altitude generate local topoclimates.

This difference in topoclimates can be clearly observed in the average rainfall distribution (Table 1). Although highly correlated, the average daily rainfall may differ strongly at short distances, e.g., rain gauges 2 and 3 are located at a mutual distance of 634 m. Although the correlation in daily rainfall is 0.92, the difference in average daily rainfall is more than 30%. Thus, rain events occur simultaneously at both locations, but the differences in topography result in a systematic bias in the total amount of rainfall at each rain gauge.

Correlation with topographical parameters

Looking at the correlation results (Table 2) it is clear that the geographical locations (east and north coordinates) have a strong impact on rainfall variability. Rainfall increases from west to east. Ningar is located more to the east than the other catchments and has significantly higher rainfall. This trend may be attributed to the increasing influence from the Amazon basin in this catchment, at least in the amount of rainfall, if not in seasonal variation. Similarly, rainfall increases from south to north. This is most likely the same trend, because most rain gauges are located around the SW–NE axis. For the topographical parameters (slope, altitude and aspect) very few significant correlations are observed. However, when topographical and geographical parameters are combined in a multiple regression model, the correlation can be increased significantly, with R^2 -values up to 0.96. The increase in accuracy of the model

Table 2 Regression results between average daily rainfall, split up per month, and topographical parameters

| | January | February | March | April | May | June | July | August | September | October | November | December |
|--|-------------|-------------|-------------|-------------|-------------|-------------|-------------|-------------|-------------|-------------|-------------|-------------|
| <i>Analysis of variance (F)</i> | | | | | | | | | | | | |
| Aspect | 7.21 | 5.41 | 18.2 | 1.28 | 0.75 | 2.44 | 3.13 | 5.42 | 5.06 | 5.12 | 3.58 | 0.12 |
| <i>Multiple regression (R²)</i> | | | | | | | | | | | | |
| Altitude | 0.02 | 0.26 | 0.01 | 0.62 | 0.06 | 0.02 | 0.00 | 0.10 | 0.04 | 0.04 | 0.54 | 0.20 |
| Slope | 0.02 | 0.11 | 0.10 | 0.00 | 0.44 | 0.09 | 0.06 | 0.05 | 0.24 | 0.24 | 0.00 | 0.05 |
| East | 0.49 | 0.84 | 0.56 | 0.03 | 0.03 | 0.39 | 0.57 | 0.30 | 0.13 | 0.09 | 0.00 | 0.43 |
| North | 0.78 | 0.64 | 0.82 | 0.04 | 0.00 | 0.65 | 0.79 | 0.69 | 0.28 | 0.18 | 0.13 | 0.22 |
| Altitude + north + east | 0.82 | 0.85 | 0.85 | 0.69 | 0.08 | 0.70 | 0.79 | 0.86 | 0.34 | 0.23 | 0.76 | 0.53 |
| Aspect + north + east | 0.81 | 0.90 | 0.89 | 0.62 | 0.20 | 0.75 | 0.83 | 0.87 | 0.39 | 0.34 | 0.76 | 0.50 |
| Slope + north + east | 0.81 | 0.87 | 0.87 | 0.62 | 0.60 | 0.85 | 0.93 | 0.96 | 0.54 | 0.42 | 0.76 | 0.50 |

Aspect was treated as a qualitative factor with four levels (N, S, E, W). Significant correlations (at a 95% confidence level) are indicated in bold.

suggests that the topographical parameters are important at a catchment level, but this impact is insignificant at a regional level, due to regional fluctuations in average rainfall. In September, October and December, no significant correlation could be found. These are the driest months in both the coastal region and the Amazon basin. During this time, rainfall seems to be more erratic, with less significant trends. The reason for this behaviour, and therefore the mechanisms influencing rainfall generation during the dry period, is still largely unknown.

Comparison with other páramo regions

Although studies about rainfall data from the south Ecuadorian páramo are nearly non-existent, some studies describe

the annual and seasonal rainfall patterns in other páramos. An overview of the Andes is given by Sarmiento (1986). Witte (1994, 1996) and Rangel (2000) describe in detail a transect through the Colombian Cordillera Central near Bogotá (Parque de los Nevados), while Herrera (2005) describes the climate of the Costa Rican páramo. A summary of these studies is given in Table 3. Comparing this table with the results of the current study (Table 1, Fig. 5) reveals some interesting differences. The south Ecuadorian páramo has a rather low average monthly rainfall (between 85 and 130 mm month⁻¹), but compared to other páramo locations with a similar average monthly rainfall, the minima are much higher (>40 mm month⁻¹, compared to <10 mm month⁻¹ in several locations, e.g., Laguna de Otun, Pico de Aguila (Table 3)). As a result, the seasonal variability

Table 3 Average, minimum and maximum monthly rainfall at other páramos as found in the literature

| Location | Source | Altitude (m asl) | Mean (mm) | Min (mm) | Max (mm) | Seasonality |
|--------------------------------|--------|------------------|-----------|----------|----------|-------------|
| Cerro de la Muerte, Costa Rica | 1 | 3365 | 211.2 | 25 | 386 | Unimodal |
| Mucubají, Venezuela | 2 | 3550 | 80.7 | <20 | 150 | Unimodal |
| Pico del Aguila, Venezuela | 2 | 4118 | 72.4 | <10 | 120 | Unimodal |
| Monserate, Colombia | 2 | 3125 | 100.7 | 50 | 180 | Bimodal |
| La Sierra, Colombia | 3 | 3750 | 102.2 | 15 | 233 | Bimodal |
| Laguna del Otun, Colombia | 3 | 4000 | 74.4 | 4 | 148 | Bimodal |
| Ladera Oeste, Colombia | 3 | 4250 | 98.7 | 15 | 196 | Bimodal |
| Boqueron, Colombia | 3 | 4500 | 105.2 | 12 | 215 | Bimodal |
| Pico Paramo, Colombia | 3 | 4500 | 79.1 | 4 | 213 | Bimodal |
| La Linea, Colombia | 3 | 4500 | 106.4 | 48 | 204 | Bimodal |
| Africa Arriba, Colombia | 3 | 4250 | 121.7 | 60 | 256 | Bimodal |
| Africa Abajo, Colombia | 3 | 4000 | 155.3 | 16 | 278 | Bimodal |
| La Playa, Colombia | 3 | 3750 | 175.8 | 60 | 360 | Bimodal |
| Totarito, Colombia | 3 | 3600 | 76.4 | 3 | 203 | Bimodal |
| La Ermita, Colombia | 3 | 3250 | 258.3 | 160 | 496 | Bimodal |
| Isobamba, Ecuador | 2 | 3058 | 113.4 | 25 | 200 | Bimodal |

Sources are: (1) Herrera (2005); (2) Sarmiento (1986); (3) Witte (1994).

of the south Ecuadorian páramo is very weak, compared to most páramos, which are characterised by a clearly marked dry season. Despite a monthly minimum of 25 mm in the páramo of Cerro de la Muerte, Costa Rica, Herrera (2005) report a yearly average of 244 wet days (>0.1 mm rainfall) or 67%, which is comparable to the value obtained in this study (76%).

Finally, only Witte (1996) reports on the spatial rainfall variability, analysing the correlation of the monthly rainfall in the studied transect. No significant correlation could be found, even at a distance of 250 m, but this is probably related to the small amount of data (12 months).

Uncertainty in interpolation

Rainfall interpolation was done for the whole study region, using the data of the 14 rain gauges. Only an extract of the resulting interpolation map is given in Fig. 9, to allow for sufficient detail. The cross validation results are given in Table 4. The slope pattern strongly dominates both interpolation maps, with few visual differences between thiessen and kriging. Both methods give good results, with the accuracy of kriging being about twice as high as thiessen (Table 4). Given the clustering of the rain gauges in study region (Fig. 1), the better results of kriging are quite remarkable: the kriging range is rather short (about 4000 m), which means that few neighbouring rain gauges can be included in the estimation, thus decreasing the advantage of kriging.

In both cases, the incorporation of additional trends significantly improves the estimation accuracy (respectively, 50% and 64%). Despite the improvements in accuracy, the variance on the estimation error does not improve. On the contrary, the variance of universal kriging is considerable higher than thiessen with normalisation (0.25 vs. 0.12). These results suggest that most of the uncertainty involved in the interpolation is related to the determination of external trends. In this regard, kriging is a rather fragile method, as it relies strongly on the assumption of stationarity in the means and thus, a lack of external trends. In this study, we were able to detect some of these trends with multiple regression. Although high correlations were found, the results suggest that a better understanding of these trends may further improve rainfall interpolation.

Table 4 Cross validation results from the interpolation of the average daily rainfall

| Method | Mean error (mm) | Error variance (mm) |
|-----------------------------|-----------------|---------------------|
| Thiessen | -0.127 | 0.269 |
| Thiessen with normalisation | -0.084 | 0.120 |
| Ordinary kriging | 0.064 | 0.216 |
| Universal kriging | 0.030 | 0.254 |

In thiessen with normalisation and universal kriging, the variables *east*, *north* and *slope* were included.

Conclusions and recommendations

In this study, patterns in daily rainfall data were analysed, using data from 14 rain gauges in the western mountain range of the south Ecuador Andes. The following conclusions can be drawn:

- Rainfall in the páramo is characterised by short, frequent low volume events. A strong daily pattern can be observed, with most rainfall occurring in the afternoon, between 14 and 19 h. Seasonal patterns are very weak, with a difference in rainfall between the driest and wettest months of only 100 mm. Only 1 in 5 days is completely without rain.
- Spatial variability in rainfall is very high. Although rainfall is strongly correlated at distances of less than 4000 m, the average daily rainfall can differ more than 25% within this range. Multiple correlation analysis revealed strong regional trends, with an increase in rainfall from SW to NE. Locally, significant correlations were found with aspect, slope and altitude. These trends are significant in wet months. In the dry seasons, rainfall seems to be much more erratic.
- Kriging is more accurate for interpolation of average daily rainfall than thiessen. The incorporation of external trends improves the accuracy in both methods, but not the error variance. These results suggest that a more detailed assessment of the relation between the topography and the spatial rainfall distribution may be able to improve interpolation results.

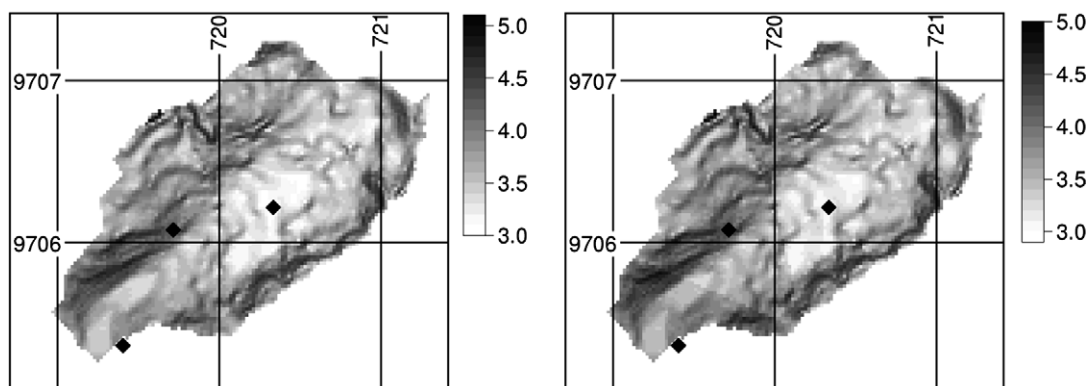


Figure 9 Extract of the interpolated map, showing the Huagrahuma catchment, using kriging (left) and thiessen (right). Few differences can be observed, as major uncertainty is related to the correlation with topography rather than the interpolation method.

The consequences for water management planning are twofold. The data presented in this study stress the need for a denser monitoring network. Currently, estimations of the total available water in the páramo, drought frequency and forthcoming minimal river flows are mostly based on a very limited number of rain gauges (e.g., Chanlud and Labrador in the northwestern Paute basin) and are therefore subject to large uncertainty. Again, the impact of topography is identified as the major source of uncertainty and is therefore recommended as a subject for further study.

Additionally, it is shown that the study region is characterised by a weak seasonal variability, compared to the páramos of Colombia, Venezuela and Costa Rica. This homogeneity is undoubtedly an important aspect of the reliability of the south Ecuadorian páramo ecosystem as a water supplier. Scientific studies, as well as testimonies of local people, suggest that climate change may increase the seasonality of the páramo climate (IDEAM, 2001; Castaño, 2002), which may result in extended drought periods and put the water supply function at risk. Assessing the seasonal variation of the páramo climate requires detailed long time datasets. However, high precision long time monitoring of the páramo climate is currently lacking but nevertheless highly recommended.

Acknowledgements

The authors thank Dr. Felipe Cisneros, director of the Program for Soil and Water Management of the Universidad de Cuenca, for the practical support, and Vicente Iñiguez, who provided valuable help during the field experiments and monitoring.

References

- Beniston, M., 2003. Climate change in mountain regions: a review of possible impacts. *Climatic Change* 59, 5–31.
- Beven, K., 2001a. How far can we go in distributed hydrological modelling? *Hydrology and Earth System Sciences* 5, 1–12.
- Beven, K.J., 2001b. *Rainfall-runoff Modelling. The Primer*. Wiley, Chichester.
- Burrough, P.A., McDonnell, R.A., 1998. *Principles of Geographical Information Systems*. Oxford University Press.
- Buytaert, W., De Bièvre, B., Wyseure, G., Deckers, J., 2005. The effect of land use changes on the hydrological behaviour of Histic Andosols in south Ecuador. *Hydrological Processes* 19, 3985–3997.
- Castaño, C., 2002. Páramos y ecosistemas alto andinos de Colombia en condición hotspot y global climatic tensor. IDEAM, Bogotá.
- ETAPA, 2004. Informe de labores 2000–2004. Technical Report, ETAPA.
- FAO, 2000. Irrigation in Latin America and the Caribbean in Figures, No. 20 in Water Report, FAO.
- Goovaerts, P., 2000. Geostatistical approaches for incorporating elevation into the spatial interpolation of rainfall. *Journal of Hydrology* 228, 113–129.
- Haan, C.T., 2002. *Statistical Methods in Hydrology*, second ed. Iowa State Press.
- Hedberg, O., 1964. Features of Afroalpine plant ecology. *Acta Phytogeographica Suecica* 49, 1–144.
- Hedberg, O., 1992. Afroalpine vegetation compared to páramo: convergent adaptations and divergent differentiation. In: Balslev, H., Luteyn, J.L. (Eds.), *Páramo: An Andean Ecosystem Under Human Influence*. Academic Press, London, pp. 15–30.
- Herrera, W., 2005. El clima de los páramos de Costa Rica. In: Kappelle, M., Horn, S.P. (Eds.), *Páramos de Costa Rica*. Instituto Nacional de Biodiversidad INBio, pp. 113–160.
- Hofstede, R., Segarra, P., Mena, P.V., 2003. Los Páramos del Mundo. Global Peatland Initiative/NC-IUCN/EcoCiencia, Quito.
- Hyndman, R.J., Grunwald, G.K., 2000. Generalized additive modelling of mixed distribution Markov models with application to Melbourne's rainfall. *Australian & New Zealand Journal of Statistics* 42, 145–158.
- IDEAM, 2001. Colombia, Primera Comunicación Nacional ante la Convención Marco de las Naciones Unidas sobre el Cambio Climático. IDEAM, Bogotá.
- IPCC, 2001. *Climate Change 2001: Impacts, Adaptation and Vulnerability*. Cambridge University Press, Cambridge.
- Jakeman, A.J., Hornberger, G.M., 1993. How much complexity is warranted in a rainfall-runoff model. *Water Resources Research* 29, 2637–2649.
- Luteyn, J.L., 1992. Páramos: why study them? In: Balslev, H., Luteyn, J.L. (Eds.), *Páramo: An Andean Ecosystem Under Human Influence*. Academic Press, London, pp. 1–14.
- Luteyn, J.L., 1999. Páramos: A Checklist of Plant Diversity, Geographical Distribution, and Botanical Literature. The New York Botanical Garden Press, New York.
- Mena, P., Medina, G., 2001. Los páramos en el Ecuador. In: Mena, P., Medina, G., Hofstede, R. (Eds.), *Los páramos del Ecuador. Proyecto Páramo*, Quito, pp. 1–24.
- Messerli, B., Viviroli, D., Weingartner, R., 2004. Mountains of the world: vulnerable water towers for the 21st century. *Ambio Special Report* 13, 29–34.
- Mitasova, H., Mitas, L., 1993. Interpolation by regularized spline with tension: I. theory and implementation. *Mathematical Geology* 25 (6), 641–655.
- Pebesma, E.J., 2004. Multivariable geostatistics in S: the gstat package. *Computers & Geosciences* 30, 683–691.
- Rangel, C., 2000. La región de vida paramuna. Colombia Diversidad Biótica III. Universidad Nacional de Colombia, Instituto de Ciencias Naturales, Bogotá.
- Sarmiento, G., 1986. Ecological features of climate in high tropical mountains. In: Vuilleumier, F., Monasterio, M. (Eds.), *High Altitude Tropical Biogeography*. Oxford University Press, Oxford, pp. 11–45.
- UAESPNN, 2000. Plan estratégico y de manejo para el Parque Nacional Natural Chingaza y su zona de influencia. Ministerio del Medio Ambiente, Republica de Colombia.
- Vuille, M., Bradley, R.S., Keimig, F., 2000. Climate variability in the Andes of Ecuador and its relation to tropical Pacific and Atlantic sea surface temperature anomalies. *Journal of Climate* 13, 2520–2535.
- Willems, P., 2001. Stochastic description of the rainfall input errors in lumped hydrological models. *Stochastic Environmental Research and Risk Assessment* 15, 132–152.
- Witte, H., 1994. Present and past vegetation and climate in the northern Andes (Cordillera Central, Colombia). Ph.D. thesis, Universiteit van Amsterdam.
- Witte, H.J.L., 1996. Seasonal and altitudinal distribution of precipitation, temperature and humidity in the Parque Los Nevados transect (Central Cordillera, Colombia). In: der Hammen, T.V., dos Santos, A.G. (Eds.), *Studies on Tropical Andean Ecosystems*, vol. 4. Cramer, Berlin, pp. 279–328.